

Discovering Power Grid Dynamics from Data Using Low-Rank Sparse Modeling

Aiman Mushtaq Purra* Danish Rafiq*

December 8, 2025

Abstract

The growing integration of renewable energy sources has significantly reduced grid inertia, making modern power systems more vulnerable to instabilities. Accurate estimation of dynamic parameters such as inertia constants and damping coefficients is critical, yet traditional model-based methods struggle with scalability and adaptiveness in large, low-inertia networks. This paper presents a novel data-driven framework that integrates Singular Value Decomposition (SVD) with Sparse Identification of Nonlinear Dynamics (SINDy) to estimate system parameters directly from time-series data. By reducing dimensionality before applying sparse regression, the proposed Latent-SINDy (L-SINDy) method mitigates overfitting while preserving essential system dynamics. The framework is validated on IEEE benchmark systems, including the 118-bus, 300-bus, and a large-scale 2869-bus European grid. The results demonstrate an accurate recovery of the inertia and damping values, with identified models that closely match the true dynamics of the system. The approach offers scalability, interpretability, and computational efficiency, highlighting its potential for real-time monitoring and control in renewable-rich grids.

Keywords: Power System Dynamics, Nonlinear Systems, Surrogate modeling

1 Introduction

1.1 Problem Statement

The increasing penetration of renewable energy sources in modern power systems is fundamentally transforming grid dynamics [1]. Conventional synchronous generators inherently provide system inertia through their rotating masses; however, these are increasingly being replaced by inverter-based resources that lack physical inertia [2]. As a result, power systems are becoming more susceptible to frequency instabilities arising from reduced inertia [3]. Furthermore, key dynamic parameters such as the inertia constant and damping coefficient are no longer static but vary continuously with changing operating conditions [4]. The absence of accurate physical models for these evolving systems further complicates real-time modeling, analysis, and control [5]. Consequently, dynamic parameter estimation has become essential for ensuring system stability. The core challenge lies in estimating these parameters adaptively without relying on fully known physical models, thereby motivating the use of data-driven approaches capable of learning system dynamics directly from measurements [6].

A considerable body of research has addressed the challenges associated with low-inertia power systems [7, 8, 9, 10]. Nevertheless, many existing techniques either presume prior knowledge of system equations or become computationally prohibitive for large-scale networks [11]. Traditional state estimation methods are also inadequate when parameters vary frequently or remain uncertain [12]. Furthermore, most conventional modeling approaches rely heavily on detailed physical representations and fixed parameters, which often fail to capture real-time system behavior [13]. Although classical parameter estimation and machine learning-based methods have shown promise, they frequently suffer from overfitting, high computational complexity, and limited interpretability [14]. These limitations become more pronounced as system dimensionality increases. Recent studies have emphasized the importance of adaptive and scalable real-time models, particularly in systems with high renewable penetration [15]. However, most existing approaches fail to adequately capture nonlinear dynamics or scale efficiently to

*Department of Electrical Engineering, Institute of Technology, University of Kashmir, Srinagar, Jammu & Kashmir, India 190006 (aimanm1232@gmail.com, danishrafiq@uok.edu.in)

large interconnected networks [16]. Hence, there is a pressing need for interpretable, data-efficient, and reduced-order modeling frameworks capable of handling the complexity of large-scale power systems.

Accurate estimation of system parameters—specifically the inertia constants (\mathbf{H}) and damping coefficients (\mathbf{D})—is crucial for stability assessment and control design [17]. In modern grids, these parameters evolve dynamically with operating conditions [10]. Traditional model-based estimation approaches require detailed system equations and are computationally intensive, making them unsuitable for large networks [17]. The advent of Phasor Measurement Units (PMUs) provides high-resolution, time-synchronized data that offers new opportunities for data-driven modeling and parameter estimation [18, 5]. Among various data-driven techniques, sparse regression methods—particularly the Sparse Identification of Nonlinear Dynamics (SINDy) framework [19, 20]—have shown great potential in identifying governing equations directly from measurement data. However, direct application of SINDy to large-scale power systems often results in overfitting and numerical ill-conditioning [21]. This limitation underscores the need to incorporate dimensionality reduction before applying SINDy. Despite its potential, such an integrated framework has not yet been systematically explored for large-scale power grids.

To address this gap, this paper proposes a hybrid modeling framework that combines dimensionality reduction with sparse identification for dynamic parameter estimation in large-scale, low-inertia power systems. The principal contributions of this work are summarized as follows:

1. We propose a hybrid framework that integrates Singular Value Decomposition (SVD) with the SINDy algorithm for dynamic parameter estimation in low-inertia grids.
2. The proposed method is applied to large IEEE benchmark systems, including the 118, 300, and 2869-bus test cases.
3. We demonstrate that the Latent-SINDy (L-SINDy) framework achieves accurate estimation of inertia constants and damping coefficients while mitigating overfitting in high-dimensional systems.
4. We provide an open-source implementation code, in the form of MATLAB scripts, to reproduce the results of the paper.

1.2 Power system dynamical model

The swing equation is a fundamental model for analyzing the transient dynamics of synchronous generators in power systems. It describes how a generator's rotor angle and speed evolve in response to disturbances such as load variations, faults, or generator outages that disrupt the balance between mechanical input power and electrical output power. Under nominal operating conditions, the mechanical torque from the prime mover equals the electrical torque delivered to the grid, maintaining a constant rotor speed. When this balance is disturbed, the rotor accelerates or decelerates depending on whether the mechanical power exceeds or falls below the electrical power. The swing equation captures this dynamic behavior by incorporating the effects of inertia, damping, and power imbalance during system disturbances.

Mathematically, the swing equation is expressed as the nonlinear second-order differential equation:

$$\frac{2\mathbf{H}_i}{\omega_R} \ddot{\boldsymbol{\delta}}_i + \frac{\mathbf{D}_i}{\omega_R} \dot{\boldsymbol{\delta}}_i = \mathbf{F}_i - \sum_{j=1; j \neq i}^n \mathbf{K}_{ij} \sin(\boldsymbol{\delta}_i - \boldsymbol{\delta}_j - \boldsymbol{\gamma}_{ij}) \quad (1)$$

where $\boldsymbol{\delta}_i$ is the rotor angle of the i th generator, ω_R denotes the system reference angular frequency, and \mathbf{H}_i and \mathbf{D}_i represent the inertia and damping constants, respectively. The term $\mathbf{K}_{ij} \geq 0$ denotes the coupling between oscillators i and j , and $\boldsymbol{\gamma}_{ij}$ is the corresponding phase shift in this coupling. The constants \mathbf{F}_i , \mathbf{K}_{ij} , and $\boldsymbol{\gamma}_{ij}$ are derived from power flow solutions and Kron reduction [22].

Three principal modeling approaches are widely used in power system studies: the Effective Network (EN), Synchronous Motor (SM), and Structure Preserving (SP) models. These models primarily differ in their representation of loads, which affects the interpretation of \mathbf{F}_i , \mathbf{K}_{ij} , and $\boldsymbol{\gamma}_{ij}$. In the EN model, loads are treated as constant impedances. The SP model represents loads as first-order oscillators with $\mathbf{H}_i = 0$, while the SM model treats them as synchronous motors represented by second-order oscillators. The inertia constant \mathbf{H} plays a vital role in determining the rate at which a rotor responds to power imbalances—higher inertia values dampen speed deviations and enhance system stability. However, as renewable energy integration increases, system inertia naturally decreases, making the swing equation

even more critical for assessing rotor stability and maintaining overall grid reliability in modern low-inertia systems.

The remainder of this paper is organized as follows. Section 2 reviews related work on inertia reduction, model reduction, and data-driven parameter estimation. Section 3 presents the proposed Latent-SINDy (L-SINDy) framework. Section 4 details the case studies conducted on IEEE benchmark systems and discusses the corresponding results. Finally, Section 5 concludes the paper and outlines key limitations and directions for future research.

2 Related Works

A variety of methods have been developed for inertia estimation and dynamic model identification in power systems [8, 9, 10]. Classical approaches rely on analytical formulations, such as the Rate of Change of Frequency (RoCoF) or energy-based methods, and on *Kalman* filtering techniques that assume a known model structure [13]. These techniques often require prior knowledge of system parameters and are limited in their adaptability to rapidly evolving grid conditions. Dynamic State Estimation (DSE), as reviewed in [17], focuses on data-driven state tracking but still depends on parameter knowledge or full state observability.

Recent advancements in data-driven methods have introduced Physics-Informed Neural Networks (PINNs) and other Machine Learning (ML) approaches for estimating generator parameters from measurement data [16, 14]. However, such methods may exhibit slow convergence and require large datasets, particularly in low-inertia systems. On the model reduction front, techniques such as Proper Orthogonal Decomposition (POD) and Singular Value Decomposition (SVD) have been widely employed for large-scale systems. For instance, [23] compared modal, balanced, and SVD-based reduction techniques and demonstrated that reduced-order models can capture dominant electromechanical modes with significantly fewer states. Nevertheless, linear reduction methods may fail to represent nonlinear interactions in higher-order dynamics.

Related research has also focused on data-driven equivalents and dynamic aggregation. The IEEE Task Force on DSE [17] has emphasized the importance of reduced-order models for enabling scalable state estimation. Despite these developments, few studies combine model reduction with sparse regression. Recent reviews further highlight that inertia estimation in low-inertia grids remains challenging and advocate hybrid approaches that integrate physics-based and data-driven techniques [2, 7].

The Sparse Identification of Nonlinear Dynamics (SINDy) algorithm [19] performs sparse regression on a library of candidate nonlinear functions to infer governing equations directly from data. Compared to PINNs and Extended Kalman Filters (EKFs), SINDy offers lower computational complexity and better generalization to unseen conditions. It has been successfully applied to a broad range of systems, including fluid dynamics [24], optical devices [25], chemical reaction networks [26], plasma convection [27], and structural systems [28], as well as in designing model predictive controllers [29].

In addition to practical applications, several theoretical extensions of SINDy have been proposed, including formulations for identifying partial differential equation (PDE) systems [30, 6], rational nonlinearities [31], incomplete datasets [32], and models incorporating physical constraints [24]. Moreover, SINDy has been combined with deep autoencoder architectures to discover intrinsic low-dimensional coordinates through joint optimization [11]. However, its applicability to large-scale power systems has not yet been extensively explored. The following subsection reviews the SINDy methodology, while its implementation for dynamic modeling in large-scale power networks is presented in the next section.

2.1 SINDy method

Consider a nonlinear dynamical system represented in state-space form as:

$$\dot{\mathbf{x}}(t) = \mathbf{f}(\mathbf{x}(t)), \quad (2)$$

where $\mathbf{x}(t) \in \mathbb{R}^n$ is the state vector with n number of state variables, and the function $\mathbf{f}() : \mathbb{R}^n \mapsto \mathbb{R}^n$ denotes the nonlinear vector field governing the state evolution. Let m be the number of temporal snapshots and t be the time vector $t = t_1, t_2, \dots, t_m$. To approximate \mathbf{f} from data, we construct the state matrix $\mathbf{X} \in \mathbb{R}^{n \times m}$ as:

$$\mathbf{X} = \begin{bmatrix} \mathbf{x}_1(t_1) & \mathbf{x}_1(t_2) & \cdots & \mathbf{x}_1(t_m) \\ \mathbf{x}_2(t_1) & \mathbf{x}_2(t_2) & \cdots & \mathbf{x}_2(t_m) \\ \vdots & \vdots & \ddots & \vdots \\ \mathbf{x}_n(t_1) & \mathbf{x}_n(t_2) & \cdots & \mathbf{x}_n(t_m) \end{bmatrix}. \quad (3)$$

The corresponding time-derivative matrix $\dot{\mathbf{X}}$ is given by:

$$\dot{\mathbf{X}} = \begin{bmatrix} \dot{\mathbf{x}}_1(t_1) & \dot{\mathbf{x}}_1(t_2) & \cdots & \dot{\mathbf{x}}_1(t_m) \\ \dot{\mathbf{x}}_2(t_1) & \dot{\mathbf{x}}_2(t_2) & \cdots & \dot{\mathbf{x}}_2(t_m) \\ \vdots & \vdots & \ddots & \vdots \\ \dot{\mathbf{x}}_n(t_1) & \dot{\mathbf{x}}_n(t_2) & \cdots & \dot{\mathbf{x}}_n(t_m) \end{bmatrix}. \quad (4)$$

We define the library of nonlinear candidate terms as follows:

$$\Theta(\mathbf{X}) = \begin{bmatrix} | & | & | & | & | & | & | \\ 1 & \mathbf{X} & \mathbf{X}^{P_2} & \cdots & \sin \mathbf{X} & \cos \mathbf{X} & \cdots \\ | & | & | & | & | & | & | \end{bmatrix}, \quad (5)$$

where \mathbf{X}^{P_2} represent higher-order polynomial terms. For instance, the quadratic polynomial candidates are given by:

$$\mathbf{X}^{P_2} = \begin{bmatrix} \mathbf{x}_1^2(t_1) & \mathbf{x}_1(t_1)\mathbf{x}_2(t_2) & \cdots & \mathbf{x}_2^2(t_1) & \cdots & \mathbf{x}_n^2(t_1) \\ \mathbf{x}_1^2(t_2) & \mathbf{x}_1(t_2)\mathbf{x}_2(t_2) & \cdots & \mathbf{x}_2^2(t_2) & \cdots & \mathbf{x}_n^2(t_2) \\ \vdots & \vdots & \ddots & \vdots & \ddots & \vdots \\ \mathbf{x}_1^2(t_m) & \mathbf{x}_1(t_m)\mathbf{x}_2(t_m) & \cdots & \mathbf{x}_2^2(t_m) & \cdots & \mathbf{x}_n^2(t_m) \end{bmatrix}. \quad (6)$$

SINDy then represented the nonlinear system (2) in terms of the data matrix (3) and (4) as:

$$\dot{\mathbf{X}} = \Theta(\mathbf{X})\Xi, \quad (7)$$

where $\Xi \in \mathbb{R}^{p \times n}$ is a sparse coefficient matrix with each column encoding the active functions governing the dynamics of the corresponding state variable. The k th state equation can thus be written as:

$$\dot{\mathbf{x}}_k = \mathbf{f}_k(\mathbf{x}) = \Theta(\mathbf{x})^T \zeta_k \quad (8)$$

where ζ_k denotes the k th column of Ξ . Consequently, the overall system can be reconstructed as:

$$\dot{\mathbf{x}}(t) = \mathbf{f}(\mathbf{x}(t)) = \Xi^T (\Theta \mathbf{x}(t)^T), \quad (9)$$

indicating that system trajectories are represented by a sparse linear combination of nonlinear basis functions. The active coefficients in Ξ are identified by solving the following sparse regression problem:

$$\Xi = \min_{\Theta} \left\| \Theta(\mathbf{X})\Xi - \dot{\mathbf{X}} \right\|_2^2 + \lambda \|\Xi\|_1 \quad (10)$$

where the first term enforces data fidelity and the second term (ℓ_1 -regularization) promotes sparsity, ensuring that only the dominant terms are retained. This leads to a parsimonious yet accurate representation of the underlying system dynamics.

2.2 Issues in SINDy

The SINDy algorithm requires constructing the data matrix $\Theta(\mathbf{X})$, containing candidate functions (monomials, trigonometric, etc.) of the state variable $\mathbf{x} \in \mathbb{R}^n$. In power systems, the snapshot matrix \mathbf{X} is generally large due to the involvement of thousands of state variables, resulting in high dimensionality ($n \gg 1$). The large state dimension leads to factorial growth of $\Theta(\mathbf{X})$, leading to an overdetermined solution of (7) [19]. Even with scaling, a large Θ matrix imposes a heavy computational bottleneck and requires far more data samples to achieve a well-determined sparse regression. Additionally, each row of n requires a separate optimization problem to be solved (cf. eq. (8)), which immediately leads to a computationally expensive task. Thus, applying SINDy directly to power grids can lead to conditioning issues, spurious nonlinear terms that do not represent known connectivity patterns, or complete failure. Therefore, there is a strong motivation to first obtain a low-rank approximation of the original state vector \mathbf{x} using dimensionality reduction, i.e., $\mathbf{x} \approx \Phi \mathbf{z}$, where $\mathbf{z} \in \mathbb{R}^r$, $r \ll n$, and then obtain a sparse representation in terms of coefficients of \mathbf{z} . This is explained in the next section.

3 Latent-SINDy for power systems

In this section, we will describe how the SINDy method can be applied to the latent variables for power system applications. To obtain the nonlinear function (\mathbf{f} , in eq. (2)), from the power system data, we collect the state data matrix \mathbf{X} given as:

$$\mathbf{X} = \begin{bmatrix} \boldsymbol{\delta}(t_0) & \boldsymbol{\delta}(t_1) & \cdots & \boldsymbol{\delta}(t_m) \\ \boldsymbol{\omega}(t_0) & \boldsymbol{\omega}(t_1) & \cdots & \boldsymbol{\omega}(t_m) \end{bmatrix} \in \mathbb{R}^{2n_g \times t_m} \quad (11)$$

and

$$\dot{\mathbf{X}} = \begin{bmatrix} \dot{\boldsymbol{\delta}}(t_0) & \dot{\boldsymbol{\delta}}(t_1) & \cdots & \dot{\boldsymbol{\delta}}(t_m) \\ \dot{\boldsymbol{\omega}}(t_0) & \dot{\boldsymbol{\omega}}(t_1) & \cdots & \dot{\boldsymbol{\omega}}(t_m) \end{bmatrix} \in \mathbb{R}^{2n_g \times t_m}, \quad (12)$$

where m is the number of snapshots collected, n_g is the number of oscillators in the system and $\boldsymbol{\omega}$ is the angular frequency of each rotor. By the application of SVD, we obtain the following:

$$\mathbf{X} = \mathbf{U}\Sigma\mathbf{V}^T \quad (13)$$

where $\mathbf{U} \in \mathbb{R}^{n \times n}$ and $\mathbf{V} \in \mathbb{R}^{t_m \times t_m}$ are orthogonal matrices and $\Sigma \in \mathbb{R}^{n \times t_m}$ is a matrix with real, non-negative entries on the diagonal and zeros off the diagonal. The entries of Σ , i.e., $\sigma_1, \sigma_2, \dots, \sigma_n$ are referred to as singular values and are ordered hierarchically from most significant to least significant, i.e., $\sigma_1 > \sigma_2 > \dots > \sigma_n$. Thus, by truncating the r columns of \mathbf{U}, \mathbf{V} and Σ given as:

$$\mathbf{X} = \mathbf{U}\Sigma\mathbf{V}^T = [\mathbf{U}_r \quad \hat{\mathbf{U}}^\perp] \begin{bmatrix} \Sigma_r \\ \mathbf{0} \end{bmatrix} \mathbf{V}^T = \mathbf{U}_r \Sigma_r \mathbf{V}^T \quad (14)$$

one can obtain a low-rank approximation of \mathbf{X} if $r < n$, where the columns of $\hat{\mathbf{U}}^\perp$ span a vector space that is complementary and orthogonal to that spanned by \mathbf{U}_r . This yields the projection matrix $\Phi_r \in \mathbb{R}^{n \times r} = \mathbf{U}_r$ by retaining first r columns of \mathbf{U} . Using the projection matrix Φ , we can obtain the low-order approximation of the state vector $\mathbf{x}(t)$ as:

$$\mathbf{x}(t) \approx \Phi_r \mathbf{z}(t), \quad (15)$$

where $\mathbf{z}(t) \in \mathbb{R}^r$ is the latent state variable. Using the approximation (15) in (2), we can derive the reduced dynamical model, which we refer to as the reduced order model (ROM) of (2), given as:

$$\dot{\mathbf{z}}(t) = \Phi_r^T \mathbf{f}_r(\Phi_r \mathbf{z}(t)), \quad (16)$$

where $\mathbf{f}_r : \mathbb{R}^n \mapsto \mathbb{R}^r$ is the reduced nonlinear function. It should be noted that since \mathbf{f} and \mathbf{f}_r remain unknown, we instead obtain the reduced snapshot matrix \mathbf{Z} as:

$$\mathbf{Z} = \Phi_r^T \mathbf{X} \in \mathbb{R}^{r \times t_m}, \quad (17)$$

which is equivalent to expressing each full state-variable $\mathbf{x}(t_i)$ in the reduced orthonormal basis Φ_r . Thus, we have:

$$\mathbf{Z} = \begin{bmatrix} | & | & | & | \\ \mathbf{z}(t_1) & \mathbf{z}(t_2) & \cdots & \mathbf{z}(t_m) \\ | & | & & | \end{bmatrix}, \quad (18)$$

and its derivative matrix

$$\dot{\mathbf{Z}} = \begin{bmatrix} | & | & | & | \\ \dot{\mathbf{z}}(t_1) & \dot{\mathbf{z}}(t_2) & \cdots & \dot{\mathbf{z}}(t_m) \\ | & | & & | \end{bmatrix} \quad (19)$$

obtained as

$$\dot{\mathbf{Z}} = \Phi_r^T \dot{\mathbf{X}} \in \mathbb{R}^{r \times t_m}. \quad (20)$$

Then we perform the SINDy method on \mathbf{Z} and $\dot{\mathbf{Z}}$ to obtain the latent dynamics model as:

$$\dot{\mathbf{z}}_k = \Theta_r(\mathbf{z}^T) \boldsymbol{\beta}_k, \quad (21)$$

where $\boldsymbol{\beta}_k$ is the k th column of the reduced coefficient matrix $\Xi_r \in \mathbb{R}^{q \times r}$, q is the number of library functions used in the reduced coordinates \mathbf{z} , and

$$\Theta_{r,i} = \begin{bmatrix} | & | & | & | & | & | & | \\ 1 & \mathbf{Z} & \mathbf{Z}^{P_2} & \mathbf{Z}^{P_3} & \cdots & \sin \mathbf{Z} & \cos \mathbf{Z} & \cdots \\ | & | & | & | & | & | & | \end{bmatrix}. \quad (22)$$

To identify active terms in the latent space, we solve a sparse regression problem in Ξ_r , given as:

$$\Xi_r = \min_{\Theta_r} \left\| \Theta_r(\mathbf{Z}) \Xi_r - \dot{\mathbf{z}} \right\|_2^2 + \lambda \|\Xi_r\|_1 \quad (23)$$

Finally, we can reconstruct the full-state prediction $\hat{\mathbf{x}} \approx \Phi_r \mathbf{z}$ by integrating the identified reduced-order model (21). The above discussion is illustrated in Fig. 1 and the steps are summarized in Algorithm (1). In practice, we tune the SINDy regularization parameter λ to balance sparsity and accuracy. The latent dimension r can be chosen by inspecting the singular value decay or by cross-validation. In the next section, we will show the application of L-SINDy for power systems.

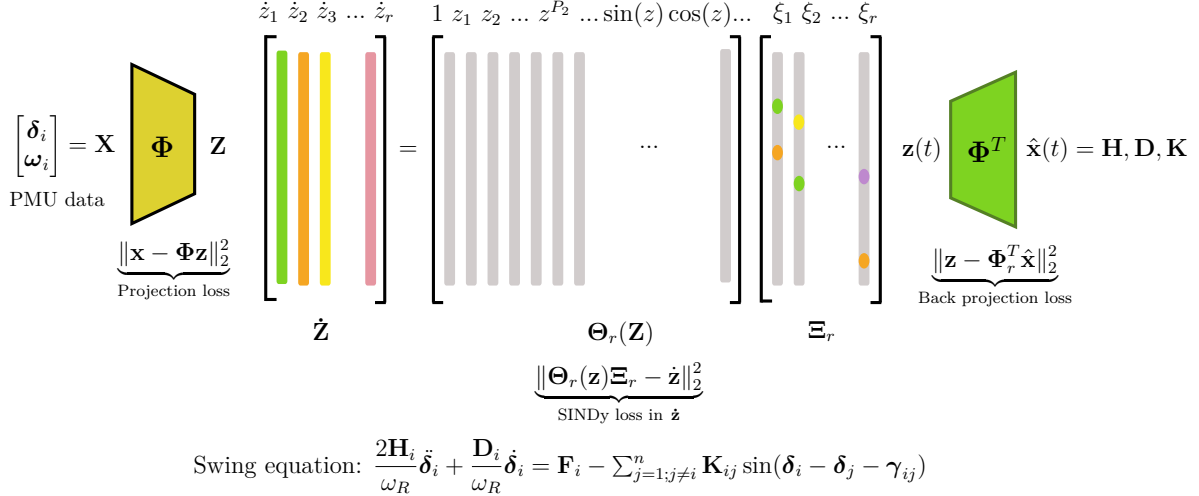


Figure 1: Graphical illustration of LSINDy

Algorithm 1 Latent Sparse Identification of Nonlinear Dynamics (L-SINDy)

Input: Rotor-angle δ_i and frequency data ω_i

Output: Sparse coefficient matrix Ξ_r , reconstructed state vector $\hat{\mathbf{x}}$

- 1: Formulate \mathbf{X} as per eqn. (11)
- 2: $[\mathbf{U}, \mathbf{\Sigma}, \mathbf{V}] = svd(\mathbf{X})$ ▷ perform SVD on \mathbf{X}
- 3: $\Phi_r = truncate(\mathbf{U})$ ▷ retain r columns of \mathbf{U}
- 4: Formulate \mathbf{Z} and $\dot{\mathbf{Z}}$ as per (18) and (19)
- 5: Construct the library Θ_{ri} as per eqn. (22)
- 6: Set tuning parameter λ
- 7: Perform sparse regression (23) to obtain Ξ_r
- 8: Solve the reduced system $\dot{\mathbf{z}} = \Theta_r(\mathbf{z}^T) \beta_k$
- 9: Back project to obtain the full state dimension $\hat{\mathbf{x}} \approx \Phi_r \mathbf{z}$

4 Numerical Simulations

We apply the proposed L-SINDy method to three test systems of increasing size: (i) *IEEE 118-bus* having 54 generators, (ii) *IEEE 300-bus* with 69 generators, and (iii) *2869-bus European high-voltage* network having 510 generators. The simulations have been performed in MATLAB version R2018a running on an 11th Gen Intel(R) Core(TM) i5-11300H @ 3.10GHz desktop computer with 32 GB RAM. All models have been simulated using MATLAB's built-in *ode45* solver [33] for a time span of [0, 5s] with a step size of $\Delta t = 0.01s$. The data was obtained from the MATPOWER library [34] to construct the EN power grid models as described in [22].

4.1 IEEE-118 Bus system

The IEEE 118 Bus model is a benchmark model comprising 118 buses and $n_g = 54$ generators. To test the L-SINDy method, $m = 500$ time snapshots were recorded, consisting of rotor angles δ_i and

corresponding frequencies ω_i of all the generators. Using the SVD on the data- matrix \mathbf{X} , we obtained the singular values. The decay of singular values and the energy captured by each singular value is presented in Figs. 2 and Fig. 3, respectively. From the figures, we can observe the slow decay of singular values, a typical characteristic of power system models. Using Algorithm 1, we identified a reduced state model of size $r = 12$ by retaining 12 dominant singular values that capture $\approx 99.9\%$ energy in the data. It should be noted that the choice of reduced dimension plays a significant role in the overall quality of the L-SINDy method. In Fig. 4, we present the comparison of all the 12 latent states against the latent states obtained by compressing the true data. As can be seen, L-SINDy correctly identifies the latent evolution of these variables. In Fig. 5, we show the time evolution of the average of all the rotor angles δ and frequency deviations $\Delta\omega$ for the true solution and the L-SINDy solution. As can be seen, L-SINDy accurately predicts the system dynamics, which is also verified from the ℓ_2 -norm errors plotted in Fig. 6 and reported in Table 1.

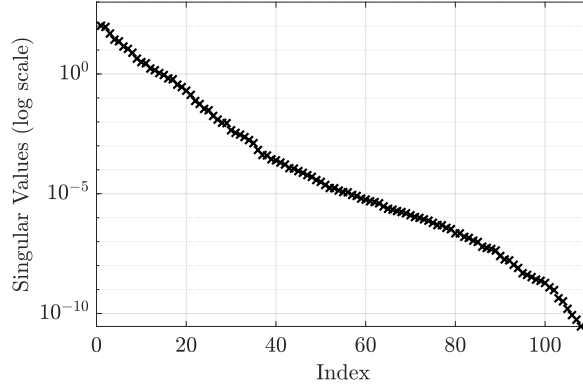


Figure 2: Singular Value decay plot of IEEE-118 bus system

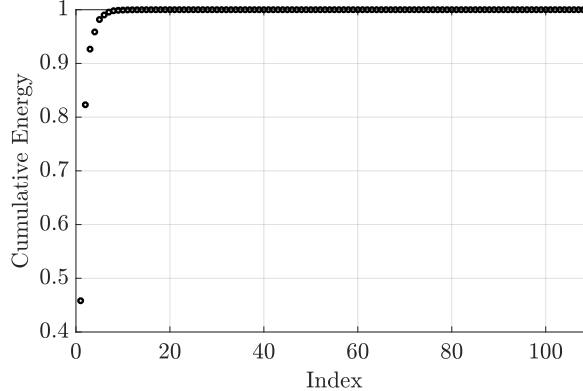


Figure 3: Singular Value energy plot of IEEE-118 bus system

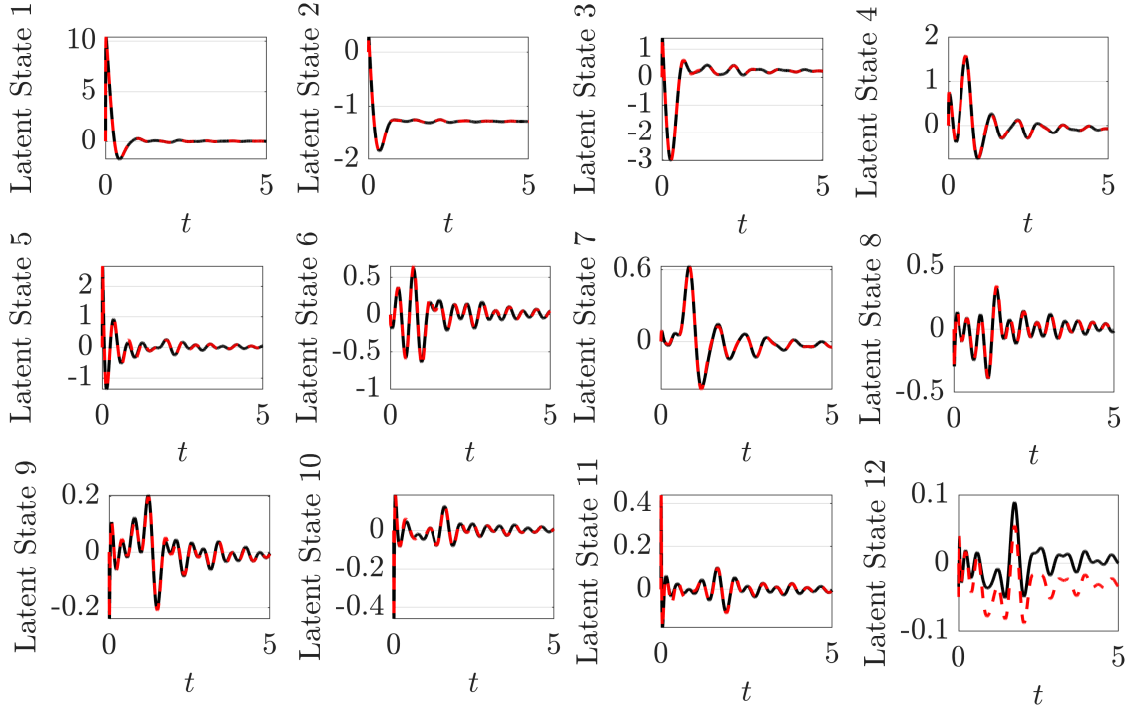


Figure 4: Original latent states and their SINDy predictions for the IEEE 118 Bus systems. The solid lines denote the actual latent states obtained by compressing the true data, and the dashed lines denote the SINDy predictions.

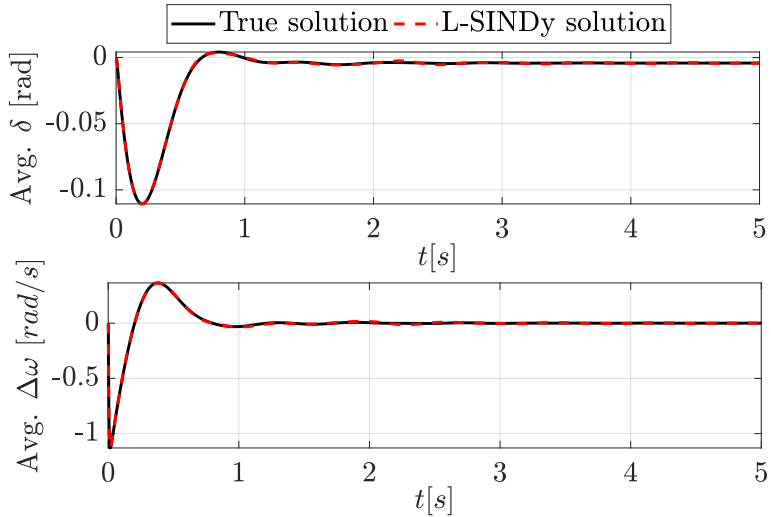


Figure 5: Comparison of true and estimated values of avg. δ and avg. $\Delta\omega$ in IEEE-118 bus system.

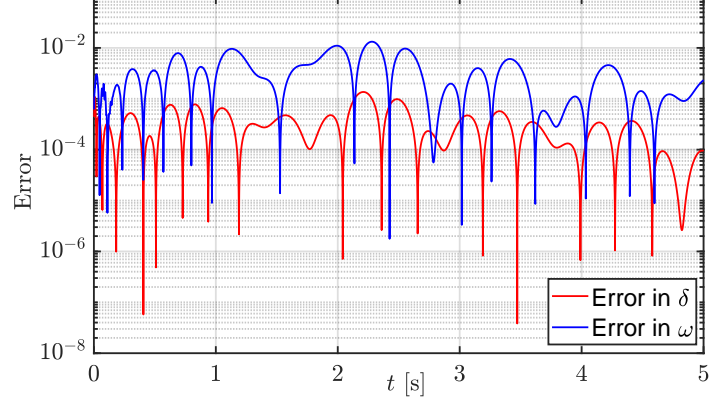


Figure 6: Error plots of the average δ and avg. ω error in IEEE-118 bus system.

4.2 IEEE-300 Bus system

Next, we used the IEEE-300 Bus system. This system represents a considerably more complex test case compared to the previous model. The decay of singular values and the energy captured for this case are shown in Figs. 7 and 8 respectively. We can observe that the system exhibits a much slower decay, necessitating a higher size of ROM. For this case, we used $r = 25$ POD modes while using Algorithm 1. The plots of latent variables are shown in Fig. 9, and the output response is presented in Fig. 10. The error plot of the output is shown in Fig. 11 and quantified in Table 1. The results indicate that the errors remain consistently small and stable over time, demonstrating the superior performance of the proposed L-SINDy method.

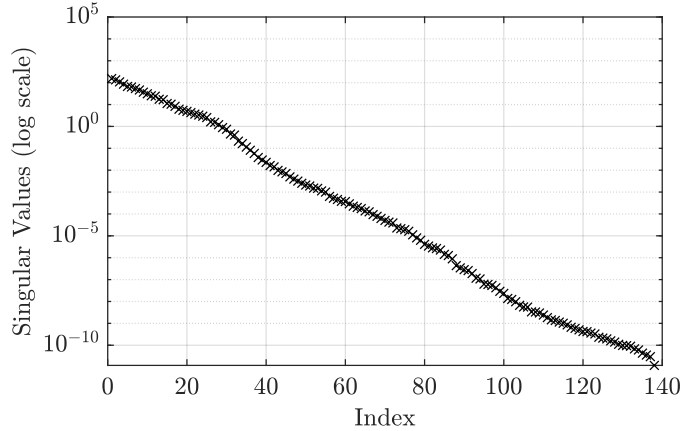


Figure 7: Singular value decay plot of IEEE-300 bus system

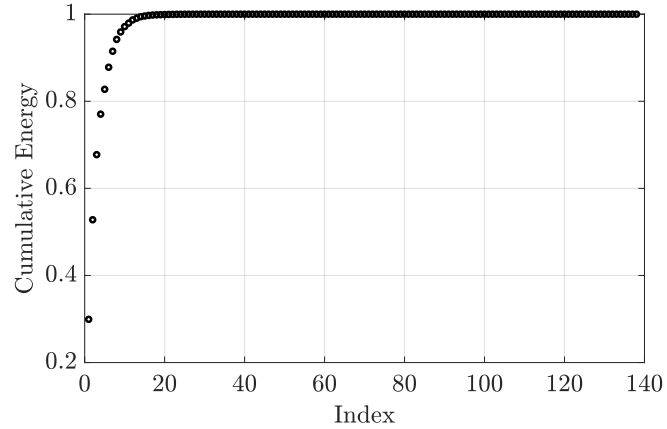


Figure 8: Singular value energy plot of IEEE-300 bus system

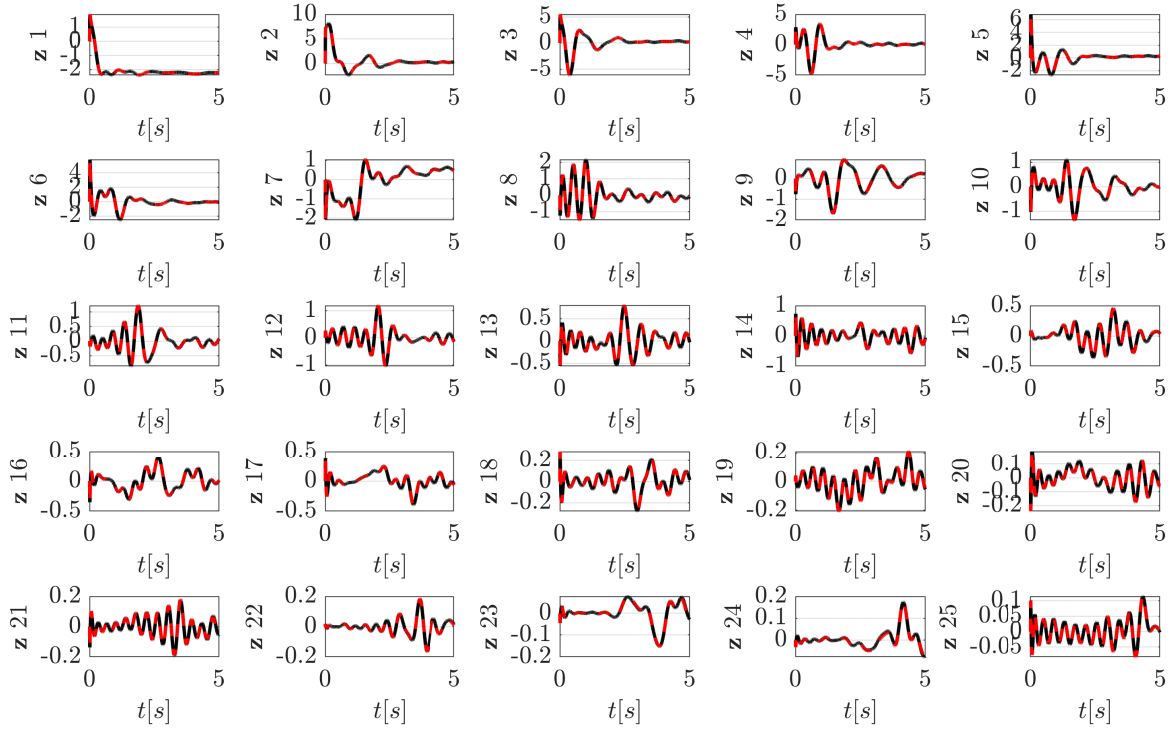


Figure 9: Original latent states and their SINDy predictions for the IEEE 300 Bus systems. The solid lines denote the actual latent states obtained by compressing the true data, and the dashed lines denote the SINDy predictions.

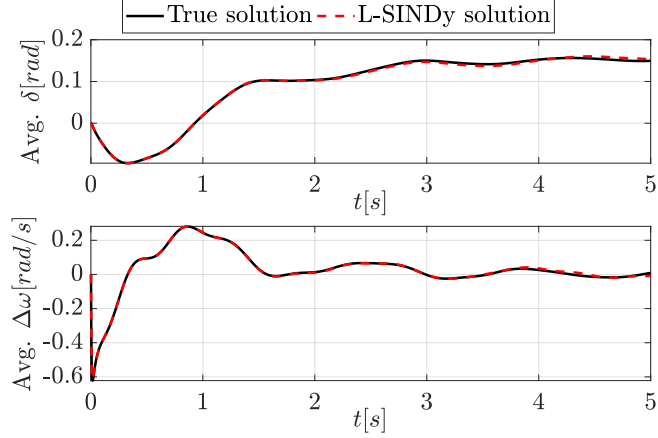


Figure 10: Comparison of true and estimated values of avg. δ and avg. $\Delta\omega$ in IEEE-300 bus system.

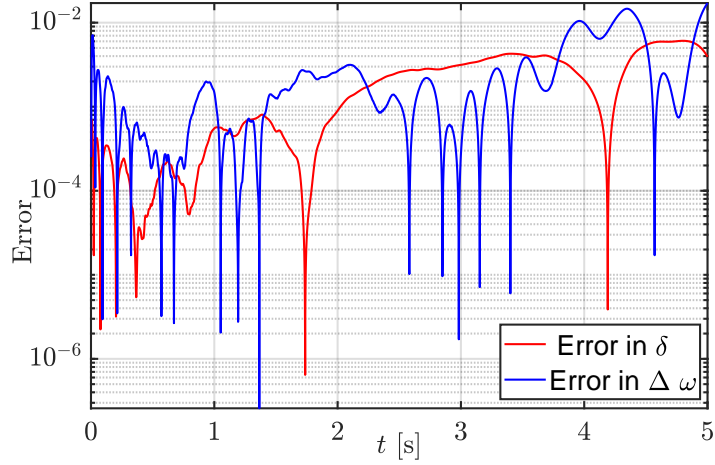


Figure 11: Comparison of avg. δ and avg. ω error in IEEE-300 bus system.

4.3 European High Voltage transmission system

Finally, to check the scalability of the proposed L-SINDy method, we used a real-sized power system. The model consists of 2869 buses and 510 generators, resulting in the model dimension of $\approx 2^{10}$. The decay of singular values and the energy captured by POD models is presented in Figs. 12 and 13 respectively. Using Algorithm 1, we determined an appropriate reduced state model of size $r = 28$ which captures $\approx 99.9\%$ energy in the system. Further analysis of the latent-state trajectories, as presented in Fig. 14, highlights how the reduced-order model captures the essential coherent patterns within the 2869-bus system. Despite the complexity and size of the network, only a small number of modes were sufficient to describe the coherent generator dynamics. The output plot showing the true and L-SINDy is shown in Fig. 15, and the corresponding error plot is shown in Fig. 16. We observe from the figures that L-SINDy can capture the strong nonlinear behavior of the system effectively. This is also verified from the relative ℓ_2 -norm errors reported in Table 1.

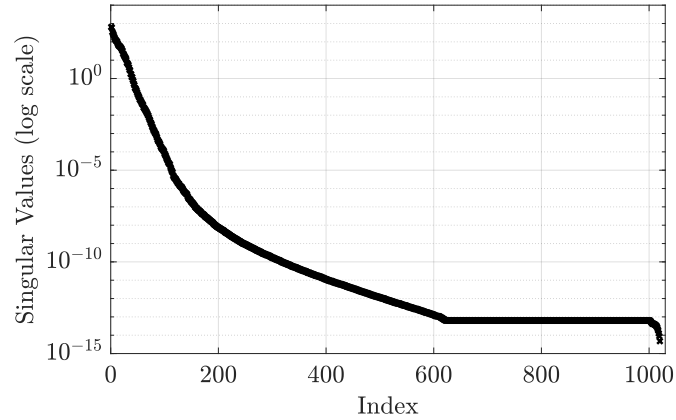


Figure 12: Singular value decay plot of European High Voltage system

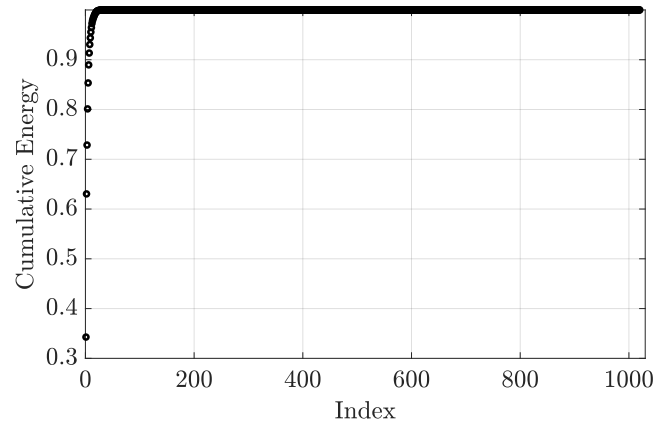


Figure 13: Singular value energy plot of European High Voltage system

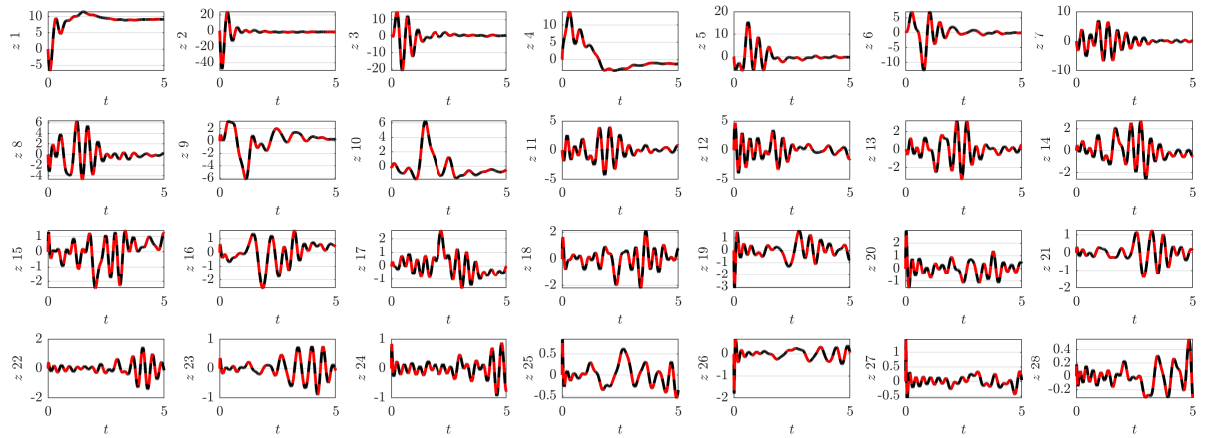


Figure 14: Original latent states and their SINDy predictions for the IEEE 2869 Bus systems. The solid lines denote the actual latent states obtained by compressing the true data, and the dashed lines denote the SINDy predictions.

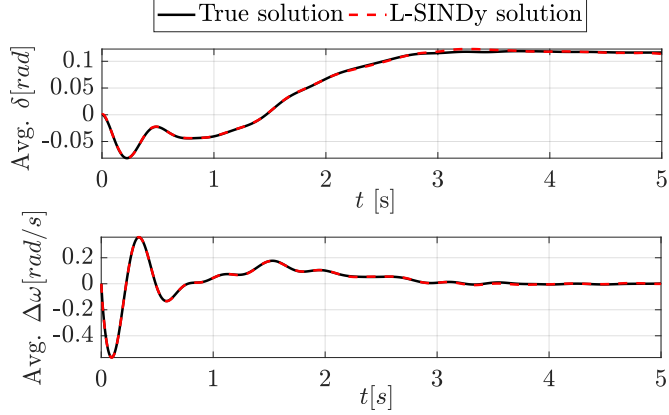


Figure 15: Comparison of true and estimated values of avg. δ and avg. $\Delta\omega$ in the European High Voltage system.

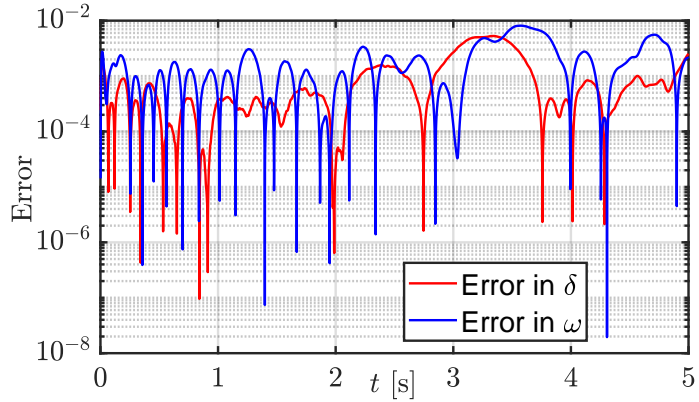


Figure 16: Comparison of avg. δ and avg. ω error in the European High Voltage system.

Table 1: Comparison of relative ℓ_2 norm errors and CPU time

Case Study	Polyorder	λ	err_δ	err_ω	FOM-Time (s)	ROM-Time(s)
IEEE 118 Bus ($n_g = 54, n = 108, r = 12$)	4	0.001	1.6×10^{-2}	3×10^{-2}	6.87	2.31
IEEE 300 Bus ($n_g = 69, n = 138, r = 25$)	1	0.001	2.3×10^{-2}	3.5×10^{-2}	8.42	4.12
IEEE 2869 Bus ($n_g = 510, n = 1020, r = 28$)	1	0.001	1.8×10^{-2}	2.3×10^{-2}	12.65	7.54

5 Conclusion and Future Work

This paper presents a novel SVD-assisted SINDy framework for estimating dynamic parameters in large-scale low-inertia power grids. By using a reduced-order modeling framework with sparse regression, the technique can identify power grid dynamics accurately and efficiently. This is achieved by solving the sparse regression problem on the reduced POD modes instead of the original state variables. This drastically reduces the size of the variables for the sparse optimization and yields significant computational savings. We demonstrate our findings on the IEEE 118-bus, 300-bus, and 2869-bus test cases. The identified sparse models closely match the true system dynamics, confirming the viability of the proposed L-SINDy method. We provide numerical algorithms and the source codes for researchers and practitioners.

The future work will involve testing the proposed scheme for renewable-rich grids, where the dynamics will evolve more rapidly. Also, the L-SINDy method can be made more robust by introducing uncertainty quantification measures to test the viability of the surrogate models during inference. Finally, integrating L-SINDy with online learning from PMU data would enable real-time monitoring of inertia changes in large-scale grids.

6 Data availability

The code to reproduce the results in this paper is freely available at GitHub: <https://github.com/DanishRaf32/LSINDy>

References

- [1] Antonio Enas, Chris Kimmett, and Jack Joyce. Inertia monitoring on renewable energy grids: Quantifying modern grid stability challenges for systems with high inverter-based resource penetration using new digital technology. *IEEE Electrification Magazine*, 10(3):55–64, 2022.
- [2] Mohamed Abouyehia, Agustí Egea-Àlvarez, and Khaled H Ahmed. Evaluating inertia estimation methods in low-inertia power systems: A comprehensive review with analytic hierarchy process-based ranking. *Renewable and Sustainable Energy Reviews*, 217:115794, 2025.
- [3] Emmanuel J Candès, Justin Romberg, and Terence Tao. Robust uncertainty principles: Exact signal reconstruction from highly incomplete frequency information. *IEEE Transactions on information theory*, 52(2):489–509, 2006.
- [4] Andreas Ulbig, Theodor S Borsche, and Göran Andersson. Impact of low rotational inertia on power system stability and operation. *IFAC Proceedings Volumes*, 47(3):7290–7297, 2014.
- [5] Theodor S Borsche, Tao Liu, and David J Hill. Effects of rotational inertia on power system damping and frequency transients. In *2015 54th IEEE conference on decision and control (CDC)*, pages 5940–5946. IEEE, 2015.
- [6] Samuel H Rudy, Steven L Brunton, Joshua L Proctor, and J Nathan Kutz. Data-driven discovery of partial differential equations. *Science advances*, 3(4):e1602614, 2017.
- [7] Abodh Poudyal, Ujjwal Tamrakar, Rodrigo D Trevizan, Robert Journey, Reinaldo Tonkoski, and Timothy M Hansen. Multiarea inertia estimation using convolutional neural networks and federated learning. *IEEE Systems Journal*, 16(4):6401–6412, 2021.
- [8] Peju Adesina Oyewole and Dilan Jayaweera. Power system security with cyber-physical power system operation. *IEEE Access*, 8:179970–179982, 2020.
- [9] Asif Hamid, Danish Rafiq, Shahkar Ahmad Nahvi, and Mohammad Abid Bazaz. Power grid parameter estimation using sparse identification of nonlinear dynamics. In *2022 International Conference on Intelligent Controller and Computing for Smart Power (ICICCS)*, pages 1–6. IEEE, 2022.
- [10] Federico Milano, Florian Dörfler, Gabriela Hug, David J Hill, and Gregor Verbić. Foundations and challenges of low-inertia systems. In *2018 power systems computation conference (PSCC)*, pages 1–25. IEEE, 2018.
- [11] Kathleen Champion, Bethany Lusch, J Nathan Kutz, and Steven L Brunton. Data-driven discovery of coordinates and governing equations. *Proceedings of the National Academy of Sciences*, 116(45):22445–22451, 2019.
- [12] Rui Luo. Unraveling low-dimensional network dynamics: A fusion of sparse identification and proper orthogonal decomposition. *arXiv preprint arXiv:2308.10458*, 2023.
- [13] Luca Rosafalco, Paolo Conti, Andrea Manzoni, Stefano Mariani, and Attilio Frangi. Ekf-sindy: Empowering the extended kalman filter with sparse identification of nonlinear dynamics. *Computer Methods in Applied Mechanics and Engineering*, 431:117264, 2024.

[14] Santosh Diggikar, Arunkumar Patil, Siddhant Satyapal Katkar, and Kunal Samad. Machine learning-based inertia estimation in power systems: a review of methods and challenges. *Energy Informatics*, 8(1):57, 2025.

[15] Diego Rodales, Alejandro Zamora-Mendez, José Antonio de la O Serna, Juan M Ramirez, Mario R Arrieta Paternina, Lucas Lugnani, Gabriel E Mejia-Ruiz, Alexander Sanchez-Ocampo, and Daniel Dotta. Model-free inertia estimation in bulk power grids through o-splines. *International Journal of Electrical Power & Energy Systems*, 153:109323, 2023.

[16] Maziar Raissi, Paris Perdikaris, and George E Karniadakis. Physics-informed neural networks: A deep learning framework for solving forward and inverse problems involving nonlinear partial differential equations. *Journal of Computational physics*, 378:686–707, 2019.

[17] Junbo Zhao, Antonio Gómez-Expósito, Marcos Netto, Lamine Mili, Ali Abur, Vladimir Terzija, Innocent Kamwa, Bikash Pal, Abhinav Kumar Singh, Junjian Qi, et al. Power system dynamic state estimation: Motivations, definitions, methodologies, and future work. *IEEE Transactions on Power Systems*, 34(4):3188–3198, 2019.

[18] Otavio Bertozzi, Harold R Chamorro, Edgar O Gomez-Diaz, Michelle S Chong, and Shehab Ahmed. Application of data-driven methods in power systems analysis and control. *IET Energy Systems Integration*, 6(3):197–212, 2024.

[19] Steven L Brunton, Joshua L Proctor, and J Nathan Kutz. Discovering governing equations from data by sparse identification of nonlinear dynamical systems. *Proceedings of the national academy of sciences*, 113(15):3932–3937, 2016.

[20] Urban Fasel, Eurika Kaiser, J Nathan Kutz, Bingni W Brunton, and Steven L Brunton. Sindy with control: A tutorial. In *2021 60th IEEE conference on decision and control (CDC)*, pages 16–21. IEEE, 2021.

[21] Rajasekhar Anguluri, Lalitha Sankar, and Oliver Kosut. Parameter estimation in ill-conditioned low-inertia power systems. In *2022 North American Power Symposium (NAPS)*, pages 1–6. IEEE, 2022.

[22] Takashi Nishikawa and Adilson E Motter. Comparative analysis of existing models for power-grid synchronization. *New Journal of Physics*, 17(1):015012, 2015.

[23] Mohammad Khatibi, Turaj Amraee, Hassan Zargarzadeh, and Mohammadreza Barzegaran. Comparative analysis of dynamic model reduction with application in power systems. In *2016 Clemson University Power Systems Conference (PSC)*, pages 1–6. IEEE, 2016.

[24] Jean-Christophe Loiseau and Steven L Brunton. Constrained sparse galerkin regression. *Journal of Fluid Mechanics*, 838:42–67, 2018.

[25] Mariia Sorokina, Stylianos Sygletos, and Sergei Turitsyn. Sparse identification for nonlinear optical communication systems: Sino method. *Optics express*, 24(26):30433–30443, 2016.

[26] Moritz Hoffmann, Christoph Fröhner, and Frank Noé. Reactive sindy: Discovering governing reactions from concentration data. *The Journal of chemical physics*, 150(2), 2019.

[27] Magnus Dam, Morten Brøns, Jens Juul Rasmussen, Volker Naulin, and Jan S Hesthaven. Sparse identification of a predator-prey system from simulation data of a convection model. *Physics of Plasmas*, 24(2), 2017.

[28] Zhilu Lai and Satish Nagarajaiah. Sparse structural system identification method for nonlinear dynamic systems with hysteresis/inelastic behavior. *Mechanical Systems and Signal Processing*, 117:813–842, 2019.

[29] Eurika Kaiser, J Nathan Kutz, and Steven L Brunton. Sparse identification of nonlinear dynamics for model predictive control in the low-data limit. *Proceedings of the Royal Society A*, 474(2219):20180335, 2018.

[30] Hayden Schaeffer. Learning partial differential equations via data discovery and sparse optimization. *Proceedings of the Royal Society A: Mathematical, Physical and Engineering Sciences*, 473(2197):20160446, 2017.

- [31] Niall M Mangan, Steven L Brunton, Joshua L Proctor, and J Nathan Kutz. Inferring biological networks by sparse identification of nonlinear dynamics. *IEEE Transactions on Molecular, Biological, and Multi-Scale Communications*, 2(1):52–63, 2017.
- [32] Hayden Schaeffer and Scott G McCalla. Sparse model selection via integral terms. *Physical Review E*, 96(2):023302, 2017.
- [33] R. Dormand J. and J. Prince P. A family of embedded runge–kutta formulae. *Journal of Computational and Applied Mathematics*, 6(1):19–26, 1980.
- [34] Ray Daniel Zimmerman, Carlos Edmundo Murillo-Sánchez, and Robert John Thomas. Matpower: Steady-state operations, planning, and analysis tools for power systems research and education. *IEEE Transactions on power systems*, 26(1):12–19, 2010.